ADVANCED MATERIALS
www.advmat.de

Liquid-Crystalline Elastomer Microvalve for Microfluidics

Antoni Sánchez-Ferrer, Tamás Fischl, Mike Stubenrauch, Arne Albrecht, Helmut Wurmus, Martin Hoffmann, and Heino Finkelmann*

Microvalves, as well as pumps and sensors, are some of the most crucial components in microfluidics when flow has to be controlled.[1] New developments in microvalves for microfluidics are looking at reducing the device size, holding higher pressures, improving the time response, and ensuring the biocompatibility of the components and the technology used for the manufacturing.[2–4] The most common active microvalves for flow control are based on mechanical actuators (e.g. pneumatic,[5–10] thermopneumatic,[11–15] thermomechanical,[16–19] piezoelectric,[20–25] electrostatic,[26–31] electromagnetic,[32–35] electrochemical,[36,37] or capillary-force actuators)[38] in order to control/stop the flow, contain the fluid, and isolate regions in the microfluidic device.[39,40]

Stimuli-responsive polymers are of importance in the actuation field. Hydrogels exhibit a significant difference to conventional microfluidic actuators with their ability to undergo abrupt volume changes in response to the surrounding watery environment without the requirement of an external power source.[41,42] The anisotropic volume change has been reported for a polypyrrole system which changes its volume when modifying the surrounding electric field, and can block the flow rate in a fluid system in a polydimethylsiloxane (PDMS) microchannel.[43]

Anisotropic dimensional change is a fundamental property of liquid-crystalline elastomers (LCEs), and they will certainly receive more attention as the research in the field of microelectromechanical systems (MEMS) evolves.[44] The versatile properties of these materials are a result of their elastic properties, which allow for huge deformations when an external force is applied, and for a self-created state of order because of the presence of mesogenic molecules.[45] Using LCEs as actuators in microsystems provides new possibilities and challenges. The liquid-crystalline molecules (mesogenic groups) of the aligned elastomers lose their orientation with an increase in temperature, while the polymer backbone shrinks in the direction of the director.[46,47] The nature of the mesogenic molecules (nematic or smectic), the crosslinking degree (low or high density), and the connectivity of the mesogens (side-chain or main-chain) to the polymer backbone are factors that determine the change in length and the mechanical properties of LCEs.[48,49] Spherical monodisperse particles of LCEs have been obtained by using microfluidics,[50] but little work has been done on integrating LCEs in a hybrid way for the development of microsystem technology.[51–53] The new actuation method for a microvalve described here successfully combines classical silicon technology with LCE actuators for use in lab-on-a-chip devices.

In this work, we present a successful integration of an oriented nematic side-chain LCE into a silicon-based microstructured device for the use as a microvalve for microfluidics. The new actuation principle is based on the expansion of the LCE in the directions perpendicular to the director and the shrinkage in the direction parallel to the director, all of which have been considered for the design of the device, based on the actuation of the LCE from the nematic to the isotropic state.

Liquid-Crystalline Elastomer Preparation: The nematic monodomain of a side-chain LCE was synthesized following a two-step crosslinking process.[54] All details concerning the synthesis of the mesogen and crosslinker, as well as the procedure for obtaining oriented LCEs and their chemical composition is described in the Supporting Information (Scheme SI-1). The LCE sample was fully characterized by X-ray, differential scanning calorimetry, thermoelastic, and uniaxial stress-strain experiments. Thus, the mesogen's orientation and the liquid-crystalline phase, the change in length as a function of temperature, and the mechanical properties were determined (Figures SI-1, SI-2 and SI-3, Supporting Information,).

Microchip Preparation and Assembly: In order to produce a functional microvalve structure based on complementary deformations (elongation-bending and sealing of the microchamber in the direction of the flow, with shrinkage in the other direction perpendicular to the flow upon heating), a complex structure was designed and manufactured (**Figure 1**). The volumetric flow of the medium is ensured underneath the actuator (Level 3). A small backing structure on the chip, which is on the same level as the bearing surfaces for the two ends of the actuator (Level 2), then prevents buckling to the normal direction. In this way, the actuator deformation in the main direction cannot be avoided and the deformation of the LCE is compensated by an elevated channel ground (Level 1). Two identical chips were assembled together face to face in one system including the elastomer actuator in between. One part of the assembled chip has a copper circuit on its back for heating; the other one has some electric contacts for temperature measurement (backside of the microchip).

Dr. A. Sánchez-Ferrer
Food & Soft Materials Science Group
Institute of Food, Nutrition & Health
ETH Zurich, Schmelzbergstrasse 9, 8092 Zurich, Switzerland
E-mail: antoni.sanchez@agrl.ethz.ch

Dr. A. Sánchez-Ferrer, Prof. H. Finkelmann
Albert Ludwigs University
Institute for Macromolecular Chemistry
Stefan-Meier-Str. 31, 79104 Freiburg, Germany

Dr. T. Fischl, Dr. M. Stubenrauch, Dr. A. Albrecht, Prof. H. Wurmus,
Prof. M. Hoffmann
Ilmenau University of Technology
Faculty of Mechanical Engineering
Department of Micromechanical Systems
Max-Planck-Ring 14, 98693 Ilmenau, Germany

DOI: 10.1002/adma.201102277

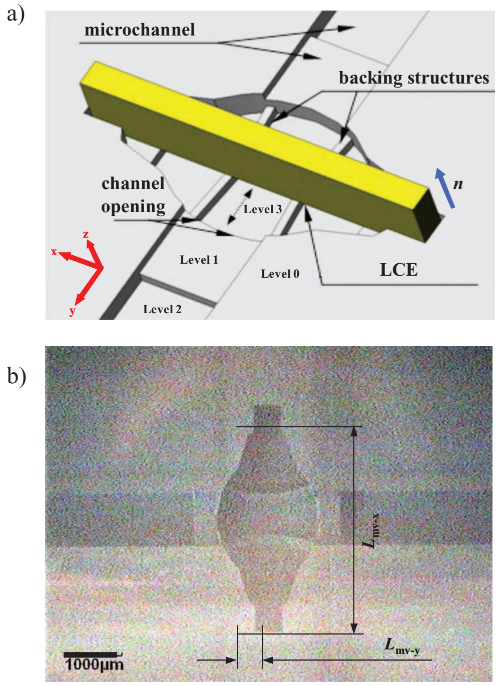

Figure 1. a) Solid model of a half of the LCE microvalve. b) Top view of the microchip before assembly.

The different levels for the microfluidic structure are transferred to the wafer in a multi-step photolithography process with subsequent etchings of the SiO_2 (wet or dry etching) (Figure SI-4, Supporting Information). The final "black-silicon" process[55] takes about 20–30 min, and the wafer thickness is reduced up to 20–30 µm. The process is a fragile equilibrium between etching and passivation in the inductive coupled plasma (ICP) process. The results are 15–20 µm needles over the whole surface of the wafer, but not on the perpendicular side walls.

The LCE was cut with a YAG-laser to the required dimensions of $0.66(L_z) \times 3.8(L_x) \times 0.30(L_y)$ mm^3. The chips were diced and the LCE was placed in the chamber at the anchor place with a predefined orientation and geometry. The distance between the actuator and the perpendicular side walls of the anchor place was about 100 to 200 µm. The two symmetric parts of the chip were joined together with the actuator inside using an external force of about 5 kN at room temperature in a hydraulic press, making it impossible to remove them one from each other without damaging the device. A platinum (Pt100) thermoresistor was placed on and glued to the surface of the chip with silver conductive glue to measure the temperature of the microchip during the experiments. The electrical contacts on the front side and on the back side of the chips were used to heat the chip with electric power and to measure the temperature of the microchip. The microchannel openings were on the side walls of the chip, and slotted plastic tubes could be fixed and glued to the openings with epoxy resin. The inlet and outlet of the chip were also sealed for gases or liquids. At present, the black-silicon technology only allows the formation of the channel opening at the side walls of the chip. Process optimization for wafers with through-holes is currently under investigation.

The dimensions of the microvalve structure after the black-silicon bonding were $10 \times 10 \times 1.04$ mm^3, with a channel size of 1×0.66 mm^2. These dimensions were chosen with respect to the thickness of the actuator and easier handling of the microchips.

Liquid-Crystalline Elastomer Microvalve: The rubber elasticity of a LCE actuator, its sealing ability, together with the anisotropic change of its length during the switching process provide an effective closing of openings in microfluidic systems. The silicon system and the LCE represent a hybrid entity without any fixed contacts between each other. The main challenge for engineering the microvalve is the bonding of the silicon system with the LCE actuator at room temperature. A new bonding technology, which can be used for silicon structures at room temperature has been reported[55] based on silicon needles, which are generated by using a modified ASE (advanced silicon etching) process in an inductively coupled plasma system. The contact of the two surfaces with black-silicon leads to a force-assisted, form-fitting bond. The purpose is to obtain a hybrid assembly of a LCE microvalve, in which the elastomer actuator can move effectively and regulate the volumetric flow rate of different mediums such as gases or liquids (e.g. water or air), in open mode at room temperature. The thermomechanical switching process in the parallel and in the perpendicular directions to the director is shown in **Fugure 2**a. Up to now, most applications with LCEs operate with the main deformation along the director ($\lambda_z = L_z/L_{zISO}$) of the actuator.[51–53]

Although the main deformation has a maximum change in length of $\lambda_z = L_z(25\ °C)/L_{zISO} = 1.46$, which corresponds to a shrinking factor of $1/\varepsilon_z = L_z(25\ °C)/L_z(90\ °C) = 69\%$, the complementary deformation perpendicular to the director in the two other directions has a maximum change in length of $\lambda_{xy} = L_{xy}(25\ °C)/L_{xyISO} = 0.83$, with its corresponding expansion factor of $1/\varepsilon_{xy} = L_{xy}(25\ °C)/L_{xy}\ (90\ °C) = 120\%$ (Figure 2b), and offers an easier assembly of the valve system. The designed anchoring place is longer and wider than the elastomer length. The cavity between the actuator and the side walls of the microstructure allows an easy mounting of the valve. If the temperature increases, the actuator provides a predefined and proportional variation of the geometry since the volume is constant ($\Delta V = 0$). Thus, the dimensions in the two directions perpendicular to the director increase, while decreasing in the main direction parallel to the alignment of the mesogens. This deformation or extension of the actuator leads to a self-clamping of the two ends of the actuator and a subsequent deformation of the LCE, which suffers an elastic buckling in the middle. This deformation is used for valve sealing in the microchamber when the actuator comes in contact with a similar shape. Figure 2c shows the switching principle of a thermomechanical actuator in a microchannel system.

Microvalve Characteristics: When the temperature increases, the LCE microvalve fills the room in the directions perpendicular to the director (L_x and L_y), up to the wall, sealing the interior of the structure. When the tension grows, an abrupt buckling of the actuator forms in the middle, and closes the microchannel. This middle part of the actuator moves to the microchamber and blocks the way of the fluid at the microchannel

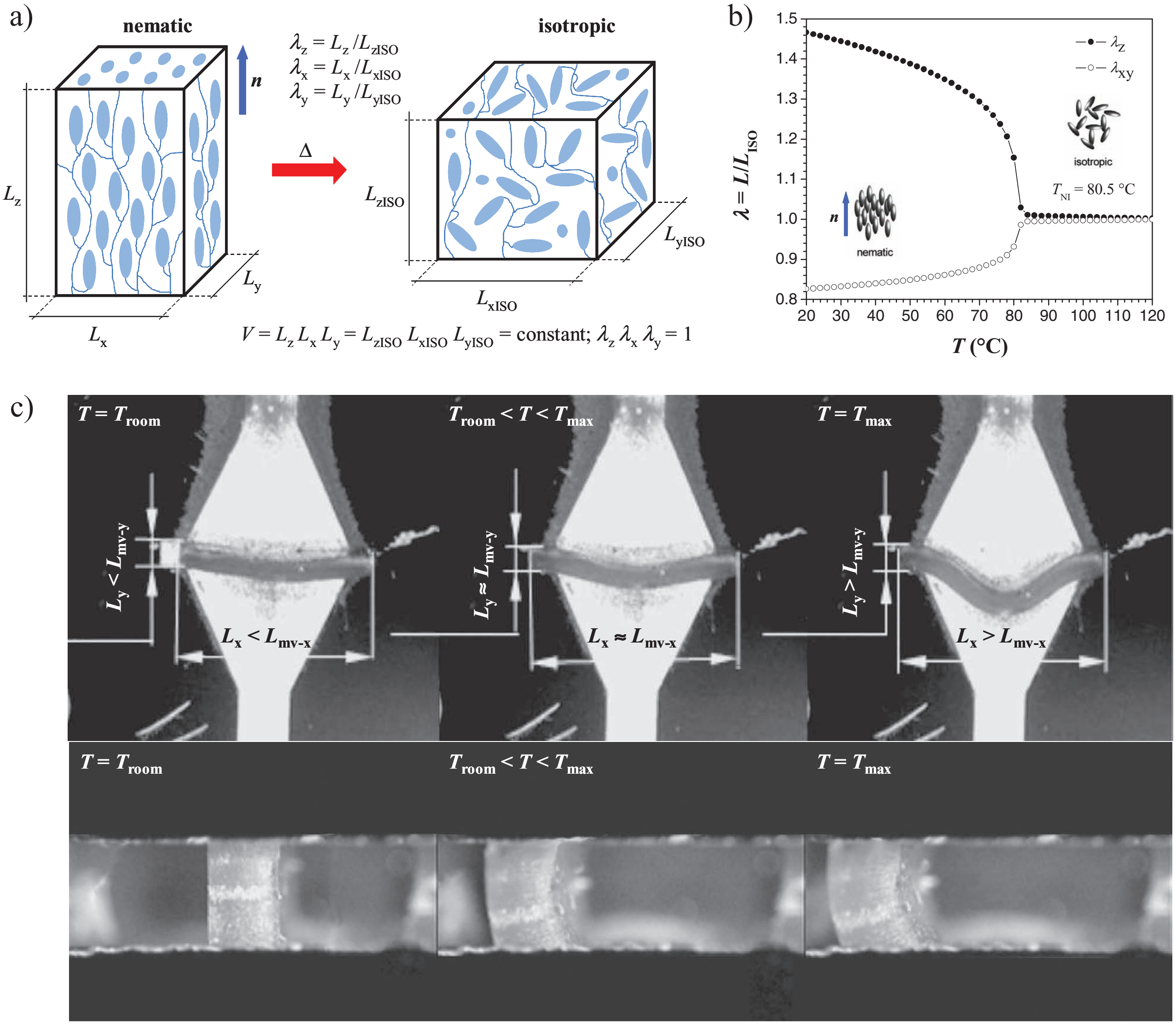

Figure 2. a) Nematic and isotropic states in a nematic side-chain LCE. b) Uniaxial parallel contraction (λ_z) and perpendicular expansion (λ_{xy}). c) Snapshot pictures during the actuation of the LCE microvalve. The actuator pushes itself at the end of the extension into the microchannel opening: moving of the microvalve-structure before the assembly of the microchip (top), and moving of the ready LCE-silicon structure through an artificial hole in one side of the chip (bottom).

opening. The actuator then creates extra pressure because of its self-clamping at the two ends in the *x*-direction. The shrinkage of the actuator in the parallel direction to the director (*z*-direction) aids its movement in the microchamber because of the friction forces being reduced between the actuator and the microstructure.

The results of the measurement are shown in **Figure 3**a–c. When the applied power increases, the temperature increases, which induces a disorder in the LCE microvalve with the consequent changes in its dimensions. At this first step, the LCE starts to expand in the *x*- and *y*-directions. When the elastomer reaches the wall of the silicon microchip, only the bending is allowed. At the same time, the expansion in the *y*-direction is sealing the microsystem, and the shrinkage in the *z*-direction and the design on the microchip finally allow the bending and closing of the microvalve. Thus an increase in the pressure is measured, together with a decrease in the flow rate as soon as the LCE is transformed into the isotropic state. When the electric power is off, the temperature starts to decrease because of the opening of the microvalve, and the exchange of heat with new water from the reservoir and the environment. Thus, the pressure falls and the flow increases again (Scheme SI-2, Supporting Information).

The maximum heating power applied by the copper electric circuit was P_{heat} = 11 W at a volumetric flow rate of water, dV_{water}/dt = 271 µL s^{-1}. This heating power was dissipated by convection and radiation to the environment (P_{diss} = 0.26 W) and also by the heat transferred to the water, dQ_{water}/dt = 10.74 W. The temperature of the water was increased in the microchip by $\Delta T = T_{outlet} - T_{inlet}$ = 9 °C. Thus, the needed electric power

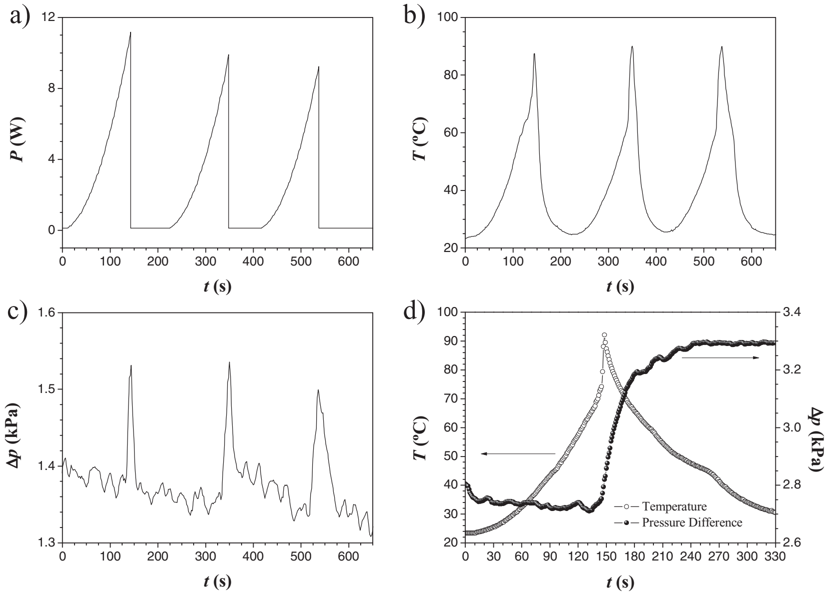

Figure 3. Characteristic LCE microvalve diagrams with water as medium (height of the reservoir $z_0 = 0.172$ m): a) heating power, b) temperature, and c) differential pressure as a function of time. d) Switching of the microvalve structure in a high pressure experiment (height of the reservoir $z_0 = 0.336$ m): the microvalve does not open during the cooling process.

was smaller when the volumetric flow rate was decreased or when a gaseous medium was used.

The differential pressure is the pressure loss in the microvalve in the steady state. When the volumetric flow rate was stopped, the measured differential pressure was the static pressure between the inlet and the outlet of the microvalve ($p_0 = \rho_{\text{water}}\, g\, z_0$; where z_0 is the height of the water reservoir).

When higher pressure, thus a higher volumetric flow rate, was applied to the microchip (Figure 3d), the LCE microvalve could not open again until reaching room temperature. As such, the microsystem can be used as a safety microvalve ($p_0 = 3.3$ kPa). Here, the dominating cooling mechanism is the heat radiation and the natural convection to the environment ($P_{\text{diss}} \neq 0$, $\mathrm{d}Q_{\text{water}}/\mathrm{d}t = 0$).

Summarizing, a new actuation principle in a microvalve has been shown that can be easily implemented in standard microsystem technologies. The new microvalve is different from the existent commercial microvalves, being based on the main actuation principle for monodomains of a LCE (change in dimensions when passing from the nematic to the isotropic state). The volumetric flow rate can be stopped just in one direction.

The hybrid integrated microvalve with a LCE as an actuator is bonded at room temperature by black-silicon bonding technology. The first prototype of the LCE microvalve of chip geometry of $10 \times 10 \times 1.04$ mm^3 can reach a switching frequency of $f = 0.01$ Hz, but different designs, the use of pulsed heating instead of continuous modes, and the improvement of LCE systems can be used to tune the volumetric flow rates and switching frequencies (down to milliseconds),[56,57] as well as to improve the efficiency of the microvalves.

This is the first time that a LCE has been used as a component for the integration of such a smart material for the elaboration of microvalves for microfluidics. Up to now, only the change in length in the direction parallel to the director has been considered of interest in monodomains of LCEs. In this work, both the expansion perpendicular to the director and the shrinkage parallel to the director are of crucial interest for the control of the microvalve.

Supporting Information

Supporting Information is available from the Wiley Online Library or from the author.

Acknowledgements

The authors acknowledge financial support from the Research Training Networks FUNCTIONAL LIQUID-CRYSTALLINE ELASTOMERS (FULCE-HPRNCT-2002-00169) and Fonds der Chemischen Industrie. They also thank Michael Hintz from the Department of Electronictechnology (Ilmenau University of Technology – Faculty for Electrotechnology and Informatics) for laser cutting of the elastomers.

Received: June 16, 2011

---

[1] N. T. Nguyen, S. T. Wereley, *Fundamentals and Applications of Microfluidics*, 2nd Edition, Artech House, Boston-London **2006.**
[2] S. Shoji, M. Esashi, *J. Micromech. Microeng.* **1994**, *4*, 157.
[3] D. Reyes, D. Iossifidis, P. A. Auroux, A. Manz, *Anal. Chem.* **2002**, *74*, 2623.
[4] P. A. Auroux, D. Iossifids, D. Reyes, A. Manz, *Anal. Chem.* **2002**, *74*, 2637.
[5] M. A. Unger, H. P. Chou, T. Thorsen, A. Scherer, S. R. Quake, *Science* **2000**, *288*, 113.
[6] K. Hosokawa, R. Maeda, *J. Micromech. Microeng.* **2000**, *10*, 415.
[7] H. Takao, M. Ishida, *J. Microelectromech. Syst.* **2003**, *12*, 497.
[8] W. H. Grover, A. M. Skelley, C. N. Liu, E. T. Lagally, R. A. Mathies, *Sens. Actuators B* **2003**, *89*, 315.
[9] S. J. Lee, J. C. Y. Chan, K. J. Maung, E. Rezler, N. Sundararajan, *J. Micromech. Microeng.* **2007**, *17*, 843.
[10] M. E. Piyasena, R. Newby, T. J. Miller, B. Shapiro, E. Smela, *Sens. Actuators B* **2009**, *141*, 263.
[11] X. Yang, C. Grosjean, Y. C. Tai, *J. Microelectromech. Syst.* **1999**, *8*, 393.
[12] K. Handique, D. T. Burke, C. H. Mastrangelo, M. A. Burns, *Anal. Chem.* **2001**, *73*, 1831.
[13] E. T. Carlen, C. H. Mastrangelo, *J. Microelectromech. Syst.* **2002**, *11*, 4080.
[14] C. A. Rich, K. D. Wise, *J. Microelectromech. Syst.* **2003**, *12*, 201.
[15] J. H. Kim, K. H. Na, C. J. Kang, D. Jeon, Y. S. Kim, *Microelectron. Eng.* **2004**, *73–74*, 864.
[16] H. P. Trah, H. Baumann, C. Döring, H. Goebel, T. Grauer, M. Mettner, *Sens. Actuators A* **1993**, *39*, 169.
[17] H. Kahn, M. A. Huff, A. H. Heuer, *J. Micromech. Microeng.* **1998**, *8*, 213.
[18] M. Kohl, D. Dittmann, E. Quandt, B. Winzek, *Sens. Actuators A* **2000**, *83*, 214.

[19] S. Vyawahare, S. Sitaula, S. Martin, D. Adalian, A. Scherer, *Lab Chip* **2008**, *8*, 1530.
[20] M. Stehr, S. Messner, H. Sandmaier, R. Zengerle, *Sens. Actuators A* **1996**, *57*, 153.
[21] N. T. Nguyen, S. Schubert, S. Richter, W. Dötzel, *Sens. Actuators A* **1998**, *69*, 85.
[22] I. Chakraborty, W. C. Tang, D. P. Bame, T. K. Tang, *Sens. Actuators A* **2000**, *83*, 188.
[23] C. K. L. Tan, M. C. Tracey, J. B. Davis, I. D. Johnston, *J. Micromech. Microeng.* **2005**, *15*, 1885.
[24] H. Kim, C. In, G. Yoon, J. Kim, *Sens. Actuators A* **2005**, *121*, 162.
[25] N. J. Graf, M. T. Bowser, *Lab Chip* **2008**, *8*, 1664.
[26] M. Shikida, K. Sato, S. Tanaka, Y. Kawamura, Y. Fujisaki, *J. Microelectromech. Syst.* **1994**, *3*, 76.
[27] N. Vandelli, D. Wroblewski, M. Velonis, T. Bifano, *J. Microelectromech. Syst.* **1998**, *7*, 395.
[28] W. van der Wijngaart, H. Ask, P. Enoksson, G. Stemme, *Sens. Actuators A* **2002**, *100*, 264.
[29] J. Xie, J. Shih, Q. Lin, B. Yang, Y. C. Tai, *Lab Chip* **2004**, *4*, 495.
[30] A. Machauf, Y. Nemirovsky, U. Dinnar, *J. Micromech. Microeng.* **2005**, *15*, 2309.
[31] A. K. Price, K. M. Anderson, C. T. Culbertson, *Lab Chip* **2009**, *9*, 2076.
[32] A. Meckes, J. Behrens, O. Kayser, W. Benecke, Th. Becker, G. Müller, *Sens. Actuators A* **1999**, *76*, 478.
[33] S. Böhm, G. J. Burger, M. T. Korthorst, F. Roseboom, *Sens. Actuators A* **2000**, *80*, 77.
[34] M. Capanu, J. G. Boyd, P. J. Hesketh, *J. Microelectromech. Syst.* **2000**, *9*, 181.
[35] T. Pan, S. J. McDonald, E. M. Kai, B. Ziaie, *J. Micromech. Microeng.* **2005**, *15*, 1021.
[36] H. Suzuki, R. Yoneyama, *Sens. Actuators B* **2003**, *96*, 38.
[37] D. E. Lee, S. Soper, W. Wang, *Microsyst. Technol.* **2008**, *14*, 1751.
[38] A. Gliere, C. Delattre, *Sens. Actuators A* **2006**, *130*, 601.
[39] K. W. Oh, C. H. J. Ahn, *Micromech. Microeng.* **2006**, *16*, R13.
[40] K. Pitchaimani, B. C. Sapp, A. Winter, A. Gispanski, T. Nishida, Z. H. Fan, *Lab Chip* **2009**, *9*, 3082.
[41] D. J. Beebe, J. S. Moore, J. M. Bauer, Q. Yu, R. H. Liu, C. Devadoss, B. H. Jo, *Nature* **2000**, *404*, 588.
[42] L. R. Hirsch, A. M. Gobin, A. R. Lowery, F. Tam, R. A. Drezek, N. J. Halas, J. L. West, *Ann. Biomed. Eng.* **2006**, *34*, 15.
[43] Y. Berdichevsky, Y. H. Lo, *Mater. Res. Soc. Symp. Proc.* **2004**, *782*, 101.
[44] S. Beeby, G. Ensell, M. Kraft, N. White, *MEMS Mechanical Sensors*, Artech House, Boston-London, **2004**.
[45] M. Warner, E. M. Terentjev, "*Liquid Crystal Elastomers*, (revised edition) Clarendon, Oxford **2007**.
[46] B. Donnio, H. Wermter, H. Finkelmann, *Macromolecules* **2000**, *33*, 7724.
[47] H. Wermter, H. Finkelmann, *e-Polymers* **2001**, no. 013.
[48] A. Sánchez-Ferrer, H. Finkelmann, *Mol. Cryst. Liq. Cryst.* **2009**, *508*, 348.
[49] A. Sánchez-Ferrer, A. Merekalov, H. Finkelmann, *Macromol. Rapid Commun.* **2011**, *32*, 672.
[50] C. Ohm, C. Serra, R. Zentel, *Adv. Mater.* **2009**, *21*, 4859.
[51] M. Bründel, M. Stubenrauch, H. Wurmus, A. Sánchez-Ferrer, *International Newsletter on Micro-Nano Integration* (MST-NEWS) **2004**, *4*, 38.
[52] T. Fischl, A. Albrecht, H. Wurmus, M. Hoffmann, M. Stubenrauch, A. Sánchez-Ferrer, *Kunststoffe* **2006**, *96*, 30.
[53] A. Sánchez-Ferrer, T. Fischl, M. Stubenrauch, H. Wurmus, M. Hoffmann, H. Finkelmann, *Macromol. Chem. Phys.* **2009**, *210*, 1671.
[54] H. Finkelmann, A. Greve, M. Warner, *Eur. Phys. J. E* **2001**, *5*, 281.
[55] M. Stubenrauch, M. Fischer, C. Kremin, S. Stoebenau, A. Albrecht, O. Nagel, *J. Micromech. Microeng.* **2006**, *16*, S82.
[56] D. K. Shenoy, D. L. Thompsen III, A. Srinivasan, P. Keller, B. R. Ratna, *Sens. Actuators A* **2002**, *96*, 184.
[57] M. Chambers, H. Finkelmann, M. Remškar, A. Sánchez-Ferrer, B. Zalar, S. Žumer, *J. Mater. Chem.* **2009**, *19*, 1524.